JOURNAL OF BACTERIOLOGY, May 1993, p. 3031–3042
0021-9193/93/103031-12$02.00/0

Vol. 175, No. 10

Characterization of *Rhodobacter capsulatus* Genes Encoding a Molybdenum Transport System and Putative Molybdenum-Pterin-Binding Proteins

GE WANG, SIEGLINDE ANGERMÜLLER, AND WERNER KLIPP*

Lehrstuhl für Genetik, Fakultät für Biologie, Universität Bielefeld, Postfach 100131, D-4800 Bielefeld 1, Germany

Received 30 November 1992/Accepted 2 March 1993

The alternative, heterometal-free nitrogenase of *Rhodobacter capsulatus* is repressed by traces of molybdenum in the medium. Strains carrying mutations located downstream of *nifB* copy II were able to express the alternative nitrogenase even in the presence of high molybdate concentrations. DNA sequence analysis of a 5.5-kb fragment of this region revealed six open reading frames, designated *modABCD*, *mopA*, and *mopB*. The gene products of *modB* and *modC* are homologous to ChlJ and ChlD of *Escherichia coli* and represent an integral membrane protein and an ATP-binding protein typical of high-affinity transport systems, respectively. ModA and ModD exhibited no homology to known proteins, but a leader peptide characteristic of proteins cleaved during export to the periplasm is present in ModA, indicating that ModA might be a periplasmic molybdate-binding protein. The MopA and MopB proteins showed a high degree of amino acid sequence homology to each other. Both proteins contained a tandem repeat of a domain encompassing 70 amino acid residues, which had significant sequence similarity to low-molecular-weight molybdenum-pterin-binding proteins from *Clostridium pasteurianum*. Compared with that for the parental *nifHDK* deletion strain, the molybdenum concentrations necessary to repress the alternative nitrogenase were increased 4-fold in a *modD* mutant and 500-fold in *modA*, *modB*, and *modC* mutants. No significant inhibition of the heterometal-free nitrogenase by molybdate was observed for *mopA mopB* double mutants. The uptake of molybdenum by *mod* and *mop* mutants was estimated by measuring the activity of the conventional molybdenum-containing nitrogenase. Molybdenum transport was not affected in a *mopA mopB* double mutant, whereas strains carrying lesions in the binding-protein-dependent transport system were impaired in molybdenum uptake.

The process of N_2 fixation has been studied for many years in a variety of different diazotrophs, and the conventional molybdenum-containing nitrogenase has been well characterized. However, it was not realized until recently that some organisms harbor, in addition to the molybdenum nitrogenase, other genetically distinct nitrogenase enzyme complexes. These alternative nitrogenases have been best characterized in the obligate aerobic soil bacterium *Azotobacter vinelandii*, which contains three distinct nitrogenase systems. The conventional nitrogenase (nitrogenase 1) includes a molybdenum cofactor, nitrogenase 2 is a vanadium enzyme, and nitrogenase 3 is a heterometal-free enzyme complex (for a review, see reference 5). The phototrophic purple bacterium *Rhodobacter capsulatus* harbors two nitrogenase systems, corresponding to nitrogenase 1 and nitrogenase 3, whereas a vanadium-containing enzyme is apparently not present (36). The expression of alternative nitrogenases in both *A. vinelandii* and *R. capsulatus* is repressed by extremely low molybdenum concentrations, indicating that high-affinity systems are involved in gene regulation.

Molybdenum, an essential trace element, is incorporated not only into the iron-molybdenum cofactor of nitrogenase but also into the molybdopterin cofactor of all other molybdoenzymes, including nitrate reductase. Genes encoding nitrate reductase and enzymes involved in synthesis of the molybdopterin cofactor as well as components for effective molybdate transport were first analyzed in *Escherichia coli* mutants resistant to chlorate (for a review, see reference 45). Partial DNA sequence and genetic analysis of the *chlD* locus of *E. coli* indicated that these genes encode components of a molybdate transport system (21, 37, 44). Recently, a new genetic nomenclature has been adopted for genes involved in molybdenum metabolism in *E. coli* and *Salmonella typhimurium* (38). For example, genes in the *chlD* locus are now designated *mod*. The *chlD* (*modC*) gene encodes a protein highly homologous to the ATP-binding proteins of different periplasmic-binding-protein-dependent, active transport systems, and *chlJ* (*modB*) codes for a protein with properties characteristic of integral membrane proteins (21).

The structure and mechanism of bacterial periplasmic transport systems have been characterized in detail for a variety of systems (including transport of histidine, maltose, oligopeptides, ribose, phosphate, and sulfate), and a general picture of these complex, multicomponent permeases has emerged (for reviews, see references 2, 11, and 40). These transport systems consist in general of four proteins: a soluble periplasmic protein that binds the substrate with high affinity; two integral membrane proteins, which allow the formation of an entry pathway; and an ATP-binding protein, believed to couple ATP hydrolysis to the transport process. The genes encoding these components of periplasmic-binding-protein-dependent transport systems are usually organized in one transcriptional unit, and the arrangement of genes is identical for different transport systems. The gene encoding the precursor of the binding protein that is cleaved during transport to the periplasm is followed by two genes encoding transmembrane proteins. The integral membrane proteins of different transport systems show extensive sim-

* Corresponding author.

TABLE 1. Bacterial strains and plasmids

Strain or plasmid	Relevant characteristics	Source or reference
R. capsulatus		
B10S	Spontaneous Sm^r mutant of *R. capsulatus* B10	22
AnfA$^-$	Derivative of *R. capsulatus* B10S carrying an *anfA*::Spc insertion	K. Schüddekopf
E. coli		
JM83	Host for pUC and pSVB plasmids	49
S17-1	RP4-2 (Tc::Mu) (Km::Tn*7*) integrated in the chromosome	41
Plasmids		
pHP45Ω	Ap^r Spc^r	30
pSUP202	Ap^r Tc^r Cm^r *mob*	41
pSVB plasmids	Ap^r Lac$^+$	4
pTn*5*-B13	pBR325::Tn*5*-B13	42
pUC plasmids	Ap^r Lac$^+$	49, 53
pUS320	Δ*nifHDK*::Km	36
pWKR56	Tc^r Km^r *mob*	22
pWKR189	Ap^r Gm^r	27
pWKR279	Δ($nifA_{II}$, $nifB_{II}$)::Km (Fig. 1)	25
pKS36	Derivative of pUS320, Δ*nifHDK*::Spc[a] (Fig. 1)	K. Schüddekopf
pWKR339	Derivative of pSUP202 carrying a 2.1-kb *Hin*dIII fragment (Spc) from pHP45Ω	This work
pWKR380B	4.4-kb *Sal*I-*Bam*HI fragment of *R. capsulatus* cloned in pWKR339 (Fig. 1)	This work
pWKR381	9.2-kb *Cla*I-*Bam*HI fragment of *R. capsulatus* cloned in pWKR56 (Fig. 1)	This work
pWKR392A	3.2-kb *Sal*I-*Hin*dIII fragment of *R. capsulatus* cloned in pUC19 (Tc^r *mob*)[b] (Fig. 1)	This work
pWKR392C	1.2-kb *Hin*dIII-*Bam*HI fragment of *R. capsulatus* cloned in pUC19 (Tc^r *mob*) (Fig. 1)	This work
pWKR392G	3.0-kb *Pst*I-*Bam*HI fragment of *R. capsulatus* cloned in pUC19 (Tc^r *mob*) (Fig. 1)	This work
pWKR420E	7.3-kb *Sal*I-*Eco*RI fragment of *R. capsulatus* cloned in pUC9 (Tc^r *mob*)	This work
pWKR423AI/II[c]	pWKR420E *mopA*::Gm (Fig. 3)	This work
pWKR423BI/II	pWKR420E *mopB*::Gm (Fig. 3)	This work
pWKR423CI/II	pWKR420E Δ(*mopA mopB*)::Gm (Fig. 3)	This work
pWKR431	1.8-kb *Pst*I-*Hin*dIII fragment of *R. capsulatus* cloned in pUC8 (Tc^r *mob*)	This work
pWKR432I/II	pWKR431 *modB*::Gm (Fig. 3)	This work
pWKR433	2.8-kb *Sal*I-*Eco*RI fragment of *R. capsulatus* cloned in pSVB28 (Tc^r *mob*)	This work
pWKR434AI/II	pWKR433 *modC*::Gm (Fig. 3)	This work
pWKR434BI/II	pWKR433 *modD*::Gm (Fig. 3)	This work
pWKR437	3.0-kb *Pst*I-*Bam*HI fragment of *R. capsulatus* cloned in pSVB21 (Tc^r *mob*)	This work
pWKR438I/II	pWKR437 *modA*::Gm (Fig. 3)	This work

[a] A DNA fragment carrying Spc^r derived from pHP45Ω.
[b] A DNA fragment carrying Tc^r and *mob* derived from pTn*5*-B13.
[c] Roman numerals refer to the orientation of the interposon.

ilarities in secondary structure but only limited amino acid sequence homologies. In contrast, the ATP-binding proteins, which are encoded by the fourth gene of the corresponding operons, exhibit a high degree of amino acid sequence similarity regardless of the transport system with which they are associated.

In this report, we present data on the DNA sequence and mutational analysis of *R. capsulatus* genes encoding a binding-protein-dependent molybdate transport system. According to the new nomenclature, we called these genes *modA*, *modB*, *modC*, and *modD*. In addition, two genes (*mopA* and *mopB*) which code for proteins containing domains homologous to molybdenum-pterin-binding proteins (Mop) were analyzed. The possible functions of *mod* and *mop* gene products in molybdenum repression of the alternative nitrogenase and in molybdenum uptake are discussed.

MATERIALS AND METHODS

Strains. The bacterial strains and plasmids used are listed in Table 1.

Media and growth conditions. The growth conditions, media, and antibiotic concentrations used to cultivate *E. coli* and *R. capsulatus* strains were described previously (22, 26, 27). To remove traces of molybdenum, the media were treated with activated carbon as described by Schneider et al. (35).

DNA sequencing. To determine an overlapping DNA sequence on both strands, appropriate restriction fragments were cloned into pSVB plasmids, and nested deletion derivatives were isolated with the exonuclease III deletion kit (Pharmacia) in both directions. Sequencing was performed by the chain termination method (34).

Construction of *R. capsulatus* insertion and deletion mutants. To construct defined *R. capsulatus* mutants, the wild-type DNA fragments listed in Table 1 and Fig. 3 were cloned by standard methods (33) into mobilizable vector plasmids, and suitable restriction sites (see Fig. 2) were used to insert DNA fragments carrying appropriate antibiotic resistance genes. The resulting hybrid plasmids (Table 1) were mobilized from *E. coli* S17-1 into *R. capsulatus* by filter matings (22), and the homogenotization of the corresponding insertion or insertion-deletion mutations was selected by the antibiotic resistance mediated by the interposon. Loss of the vector-encoded antibiotic resistance was used to identify strains carrying double cross-over events.

Complementation analysis. To complement the *R. capsulatus nifHDK-*$nifA_{II}$/$nifB_{II}$ double deletion mutant, different restriction fragments (Fig. 1) were cloned into mobilizable vector plasmids (Table 1) and conjugationally transferred

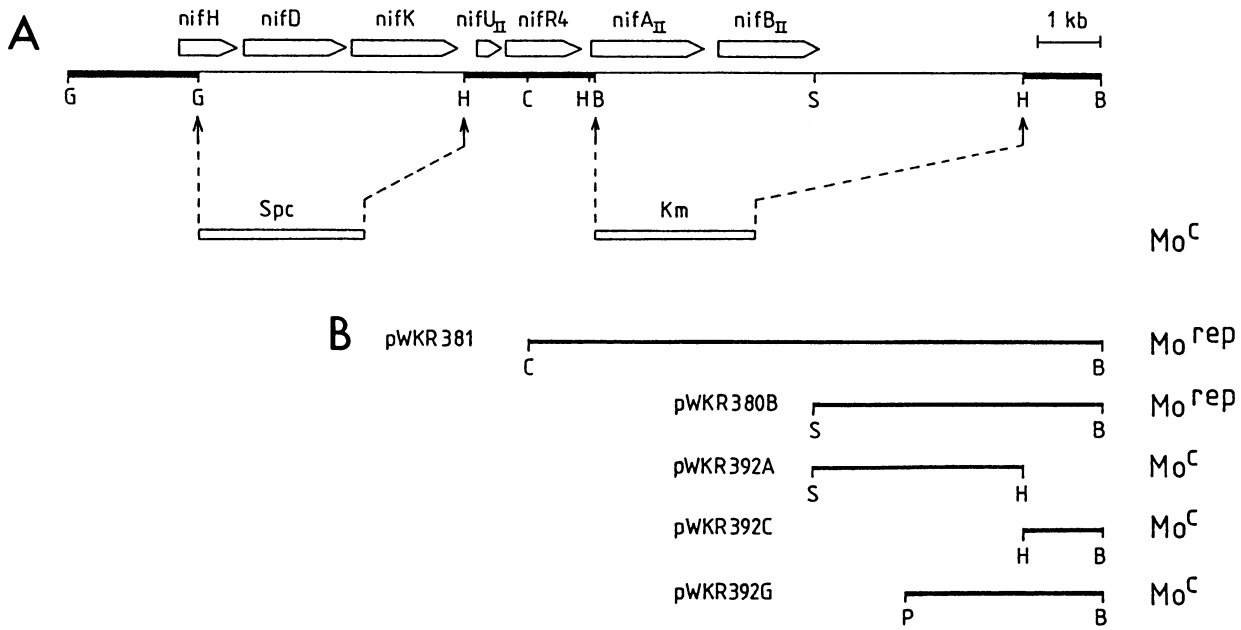

FIG. 1. Mapping of *R. capsulatus* genes involved in molybdenum repression of the alternative nitrogenase. (A) Physical map of *nif* region B (22) and locations of genes (open arrows). Interposon-induced deletions of *nifHDK* and a gene region encompassing *nifA*$_{II}$ and *nifB*$_{II}$ are indicated by thin lines. The interposons mediating resistance to spectinomycin (Spc) and kanamycin (Km) are not drawn to scale. The alternative nitrogenase of the double deletion mutant is not repressed by molybdenum (Mo^c phenotype). (B) Different restriction fragments were used to complement the double mutant (for details, see Materials and Methods and Table 1), and the resulting phenotypes are shown on the right (Mo^{rep}, the alternative nitrogenase is completely repressed by molybdenum concentrations of 3 μM). Only restriction sites used for cloning are given: *Bam*HI (B), *Bgl*II (G), *Cla*I (C), *Hin*dIII (H), *Pst*I (P), and *Sal*I (S).

from *E. coli* S17-1 to *R. capsulatus*. Since these constructs are unable to replicate in *R. capsulatus*, integration of these plasmids by single cross-over recombination via homology to the *R. capsulatus* chromosome or to one of the interposons present in the double-deletion mutant could be selected by vector-encoded antibiotic resistances. The resulting strains were tested for their ability to grow diazotrophically in N-free medium containing 3 μM molybdate in microtiter plates as described previously (22).

Nitrogenase assays in vivo. To determine the nitrogenase activity, 3-ml cultures in medium containing serine and the appropriate amount of molybdate were derepressed overnight under an atmosphere of 13 ml of N_2. Acetylene reduction was determined with a Hewlett-Packard gas chromatograph (model 5890 II) with a Chrompack Alumina column, which allowed separation of acetylene, ethylene, and ethane. The formation of ethane was routinely monitored as an indication of the activity of the alternative nitrogenase.

RESULTS

Genes involved in molybdenum repression of the alternative nitrogenase are located downstream of *nifB* copy II. The alternative nitrogenase of *R. capsulatus* is repressed by molybdenum concentrations of >50 nM (36). Therefore, diazotrophic growth of a *nifHDK* deletion strain, which is unable to express the conventional molybdenum nitrogenase, could be observed only on medium treated with activated carbon to remove traces of molybdenum (35). In contrast, an *R. capsulatus* double mutant carrying a *nifHDK* deletion and also a deletion encompassing *nifA*$_{II}$/*nifB*$_{II}$ and a 3-kb DNA fragment downstream of *nifB*$_{II}$ (Fig. 1A) was able to grow diazotrophically on medium containing 3 μM molybdate. This result demonstrated that either *nifA*$_{II}$/*nifB*$_{II}$ or genes located downstream of it are involved in molybdenum repression of the alternative nitrogenase. To discriminate between these two possibilities and to localize the genes responsible for the molybdenum-independent, constitutive expression of the alternative nitrogenase (Mo^c phenotype), the double-mutant strain was complemented by plasmids carrying different restriction fragments. As shown in Fig. 1B, molybdenum repression (Mo^{rep} phenotype) could be restored not only by a large *Cla*I-*Bam*HI fragment covering the entire deleted region but also by a 4.4-kb *Sal*I-*Bam*HI fragment carrying only the 3′ end of *nifB*$_{II}$ and adjacent regions. Therefore, genes located downstream of *nifB*$_{II}$ are responsible for molybdenum repression of the alternative nitrogenase.

Genes encoding an active molybdenum transport system and two gene products with homology to molybdenum-pterin-binding proteins. The complete nucleotide sequence of a 5,520-bp DNA fragment downstream of *nifB*$_{II}$ was determined and is presented in Fig. 2. The nucleotide sequence data reported in this study will appear in the EMBL, GenBank, and DDBJ nucleotide sequence data bases under accession number L06254. According to the codon usage preference of *R. capsulatus*, six open reading frames were identified adjacent to *nifB*$_{II}$ (Fig. 3B). Four of these coding regions, designated *modA*, *modB*, *modC*, and *modD*, are closely linked. Only 5 bp separated *modA* and *modB*, the stop codon (TGA) of *modB* overlapped the start codon (ATG) of *modC*, and there were 3 bp between *modC* and *modD*. A larger distance, 34 bp, was found between *mopA* and *modA*, whereas 260 bp separated the divergently transcribed open reading frames *mopA* and *mopB*. Sequence

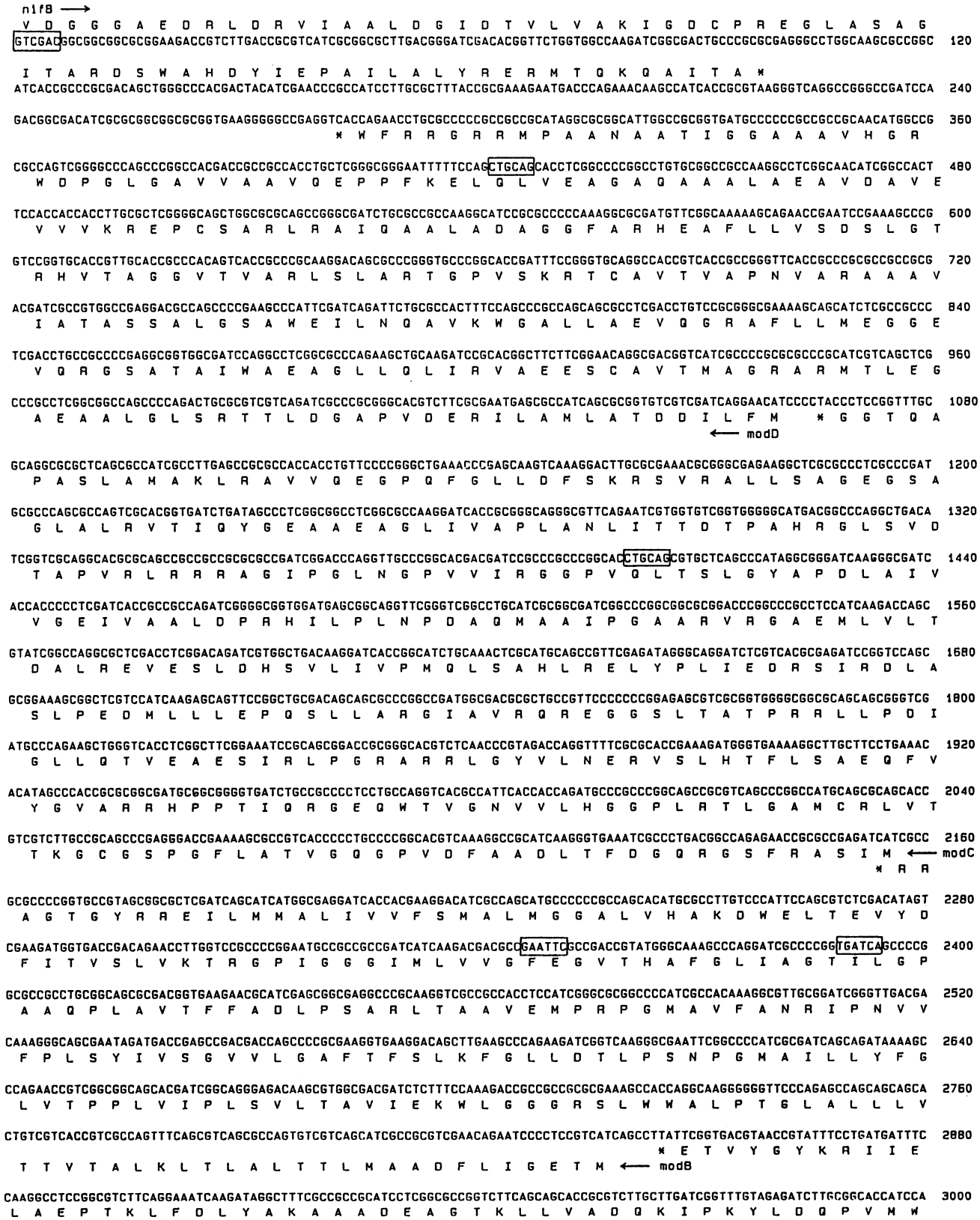

FIG. 2. Nucleotide sequence of a 5,520-bp DNA fragment located downstream of *nifB* copy II. The DNA sequence is given in the 5′→3′ direction, and the predicted amino acid sequences of *modD*, *modC*, *modB*, *modA*, *mopA*, and *mopB* are indicated in the single-letter code. Two DNA sequence motifs in front of *mopA* and *mopB* that resemble RpoN-dependent promoters are underlined with arrows, and nucleotides conforming to the −24/−12 consensus are marked by solid rectangles. Restriction sites used for the construction of insertion mutants (for details, see Table 1 and Fig. 3) are boxed.

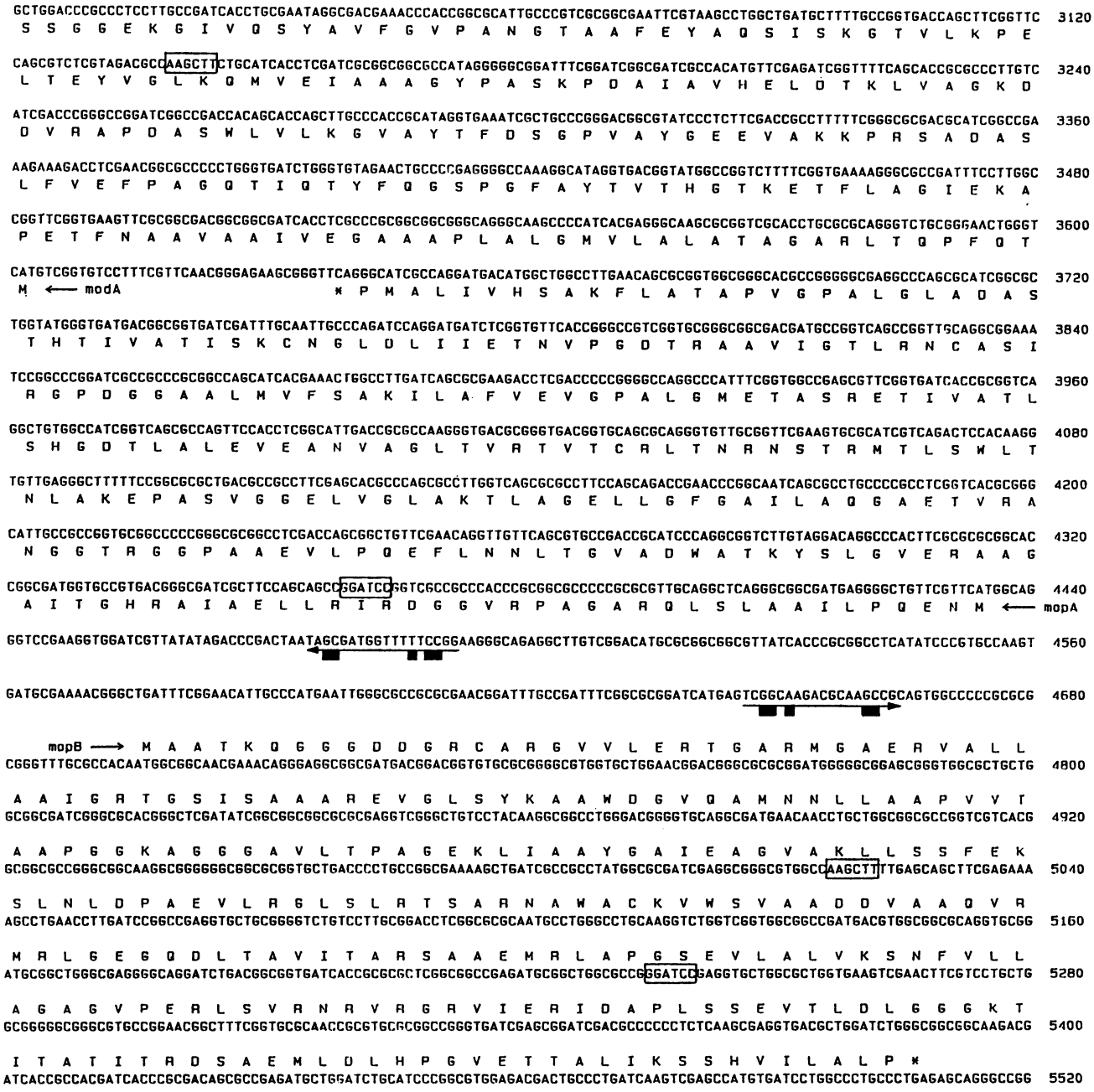

FIG. 2—*Continued.*

analysis of these two intergenic regions revealed no homology to typical procaryotic −35/−10 promoter sequences. Two sequences resembling RpoN-dependent promoters were found in front of *mopA* and *mopB* (Fig. 2). However, the sequence similarities of these putative promoter elements are restricted to the −24/−12 consensus sequence $GGNAN_8GC$, where N is any nucleotide, and no further nucleotides common to RpoN-dependent promoters (28) are conserved.

The *modC* gene encoded a polypeptide of 363 amino acid residues, with a deduced molecular weight of 38,517. As shown in Fig. 4A, the predicted amino acid sequence of *R. capsulatus* ModC exhibits a high degree of homology to that of ChlD (ModC), the ATP-binding component of the molybdate transport system of *E. coli* (21), and to ORF10, the gene product of an open reading frame located in the major *nif* cluster of *A. vinelandii* (20). A putative ATP-binding site characterized by the conserved amino acid sequence $G\text{-}X_4\text{-}G\text{-}K\text{-}S/T$ (13) is located in the N-terminal part of all three proteins (Fig. 4A). In addition to this motif, ChlD of *E. coli*, ORF10 of *A. vinelandii*, and ModC of *R. capsulatus* showed extensive sequence similarities to the ATP-binding components of a variety of periplasmic transport systems, including OppD (oligopeptide transport [14]), HisP (histidine transport [12]), and MalK (maltose transport [10]).

As shown in Fig. 4B, the gene product of *R. capsulatus*

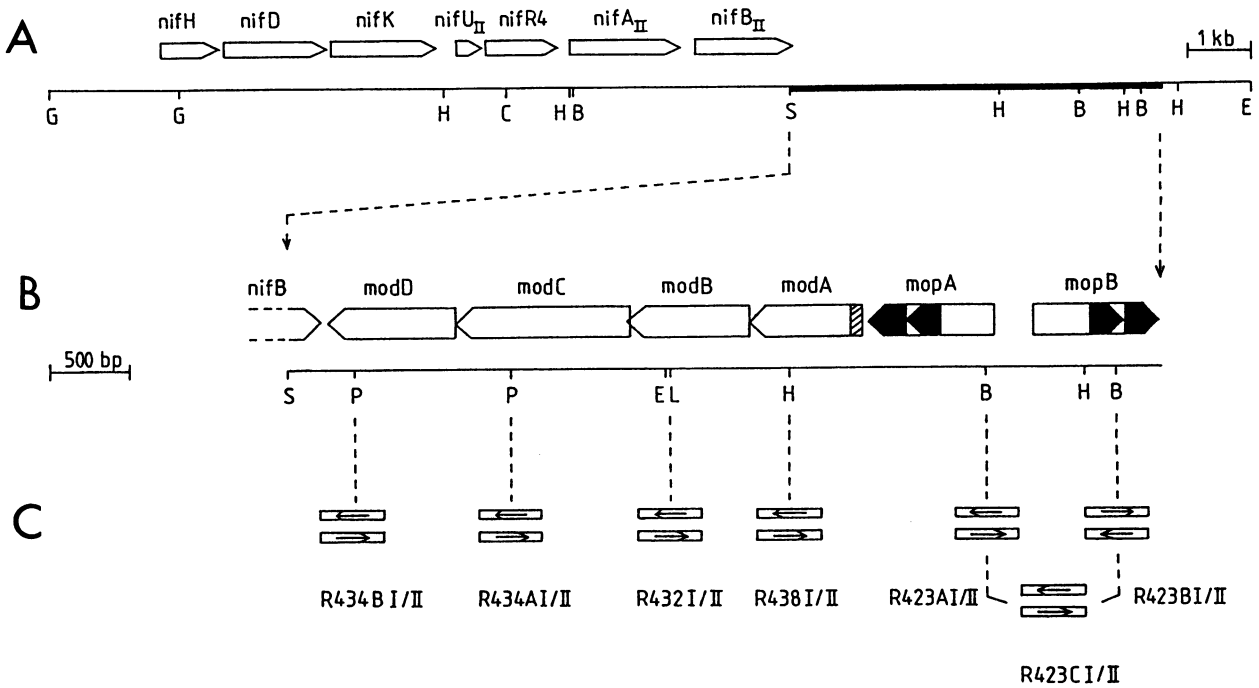

FIG. 3. Genetic organization and mutational analysis of the *R. capsulatus mod/mop* gene region. (A) The sequenced DNA fragment located downstream of *nifB*$_{II}$ is marked by a heavy line. (B) Detailed map of the sequenced region drawn at larger scale; locations of coding regions, as deduced from the nucleotide sequence, are shown by open arrows. The leader peptide of ModA is marked by a hatched bar, and the tandem repeats within MopA and MopB, which are homologous to molybdenum-pterin-binding proteins, are shown as solid arrows. (C) Locations of interposon insertions. Construction details are given in Table 1. The direction of transcription of the gentamicin resistance gene is shown with an arrow. The construction of the *mopA mopB* double deletion mutant is also shown. Interposons are not drawn to scale. Abbreviations of restriction sites are the same as in Fig. 1, plus *Bcl*I (L) and *Eco*RI (E).

modB, a protein composed of 228 amino acid residues (M_r 24,161), is homologous to ChlJ (ModB) of *E. coli* (21) and to NifC of *Clostridium pasteurianum* (51). These three proteins are characterized by several potential transmembrane segments. Using the method of Rao and Argos (31), we predicted five transmembrane helices for *R. capsulatus* ModB (marked in Fig. 4B), six membrane-spanning regions for NifC of *C. pasteurianum*, and four transmembrane elements for the 200 C-terminal amino acids available for ChlJ of *E. coli*. These secondary structures, including five or six potential membrane-spanning helices separated by short stretches of hydrophilic sequences, are typical of the integral membrane components of different transport systems (11). Although only limited overall amino acid sequence homology was found for the integral membrane proteins of different transport systems, one of the hydrophilic domains is conserved in many of these proteins (8). A high degree of sequence similarity to this motif, believed to be the site of interaction with the ATP-binding component (14), was also found in the hydrophilic stretch separating predicted transmembrane segments 3 and 4 of *R. capsulatus* ModB (Fig. 4B).

R. capsulatus modA and *modD*, coding for polypeptides of 252 amino acid residues (M_r 26,620) and 259 amino acid residues (M_r 26,782), respectively, exhibit no homology to sequences present in data bases. However, the N-terminal part of ModA contained an amino acid sequence typical of leader peptides, which are cleaved during translocation across the membrane (50). As shown in Fig. 5, all structural elements characteristic of leader sequences (two large polar glutamine residues and one positively charged arginine residue in the N-terminal region, followed by a sequence enriched in hydrophobic amino acids and a more polar C-terminal region which conforms to the "−3/−1 rule" for defining the cleavage site) are present in *R. capsulatus* ModA. Therefore, it seems likely that ModA is a periplasmic protein cleaved between the alanine and glycine residues at position 27 and 28 (Fig. 5), resulting in a mature protein with a calculated molecular weight of 23,953.

The deduced proteins encoded by *mopA* and *mopB* showed a high degree of homology to each other. The total number of amino acid residues (265 versus 270) and the calculated molecular weights (27,119 versus 27,668) are similar for MopA and MopB, and the predicted amino acid sequences showed 50% identity (Fig. 4C). An interesting feature of MopA and MopB is a tandem duplication of homologous protein domains encompassing 70 amino acid residues. As shown in Fig. 4C, these domains, located in the C-terminal part of both *R. capsulatus* proteins, exhibited extensive homologies to MopI, one of three low-molecular-weight (68 amino acid residues) molybdenum-pterin-binding proteins of *C. pasteurianum* (15, 17).

Molybdenum repression of the alternative nitrogenase influenced differently in *mod* and *mop* mutants. To determine the role of *R. capsulatus mod* and *mop* genes in molybdenum repression of the alternative nitrogenase in detail, interposon mutations in all six coding regions identified by DNA sequence analysis were constructed (Table 1, Fig. 3C). Since *mopA* and *mopB* showed a high degree of similarity to each other, indicating homologous functions, a double mutant was constructed by substituting a 0.9-kb *Bam*HI fragment with the Gm^r interposon. This interposon was previously

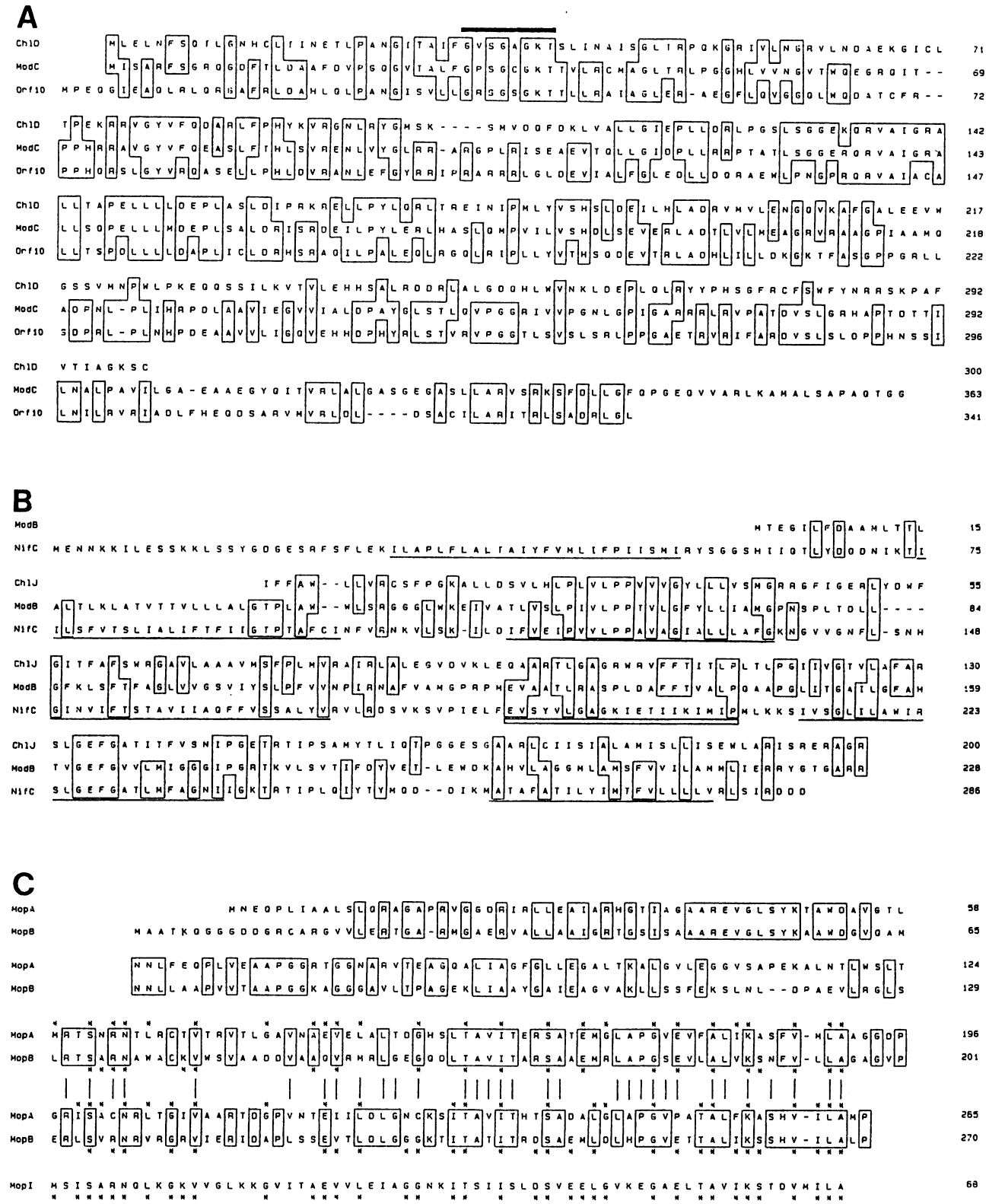

FIG. 4. Comparison of the deduced amino acid sequences of *R. capsulatus* ModC, ModB, MopA, and MopB with those of ChlD and ChlJ of *E. coli*, ORF10 of *A. vinelandii*, and NifC and MopI of *C. pasteurianum*. (A and B) Amino acid residues identical to those in the corresponding proteins of *R. capsulatus* are boxed. A putative ATP-binding site is marked by a heavy black bar. (B) The predicted transmembrane helices of ChlJ, ModB, and NifC are underlined, and a motif found in the membrane components of a variety of different transport systems (8) is marked by an open bar. (C) Amino acid residues that are identical in *R. capsulatus* MopA and MopB are boxed. To emphasize the tandem repeats present in the C-terminal parts of MopA and MopB, amino acid residues which are present in at least three of the four repeats are indicated by vertical lines. Asterisks mark amino acid residues identical to those in the molybdenum-pterin-binding protein MopI of *C. pasteurianum*.

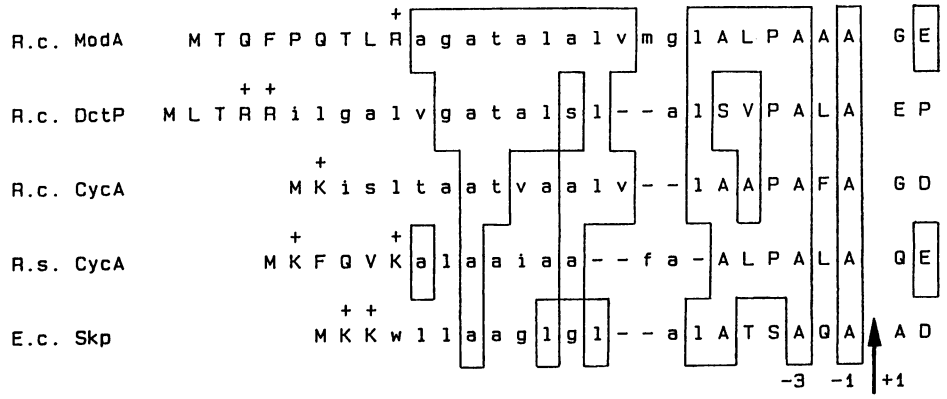

FIG. 5. Comparison of the N terminus of *R. capsulatus* (R.c.) ModA with leader sequences of the following proteins: the periplasmic C_4-dicarboxylate-binding protein (DctP) of *R. capsulatus* (39), cytochrome c_2 (CycA) of *R. capsulatus* (7) and the *R. sphaeroides* (R.s.) (9), and the *E. coli* (E.c.) (18) Skp protein. Identical amino acid residues are boxed. Positively charged amino acids in the N-terminal part are marked (+), and hydrophobic stretches of amino acid residues are shown in lowercase letters. The *E. coli* Skp protein and cytochrome c_2 of *R. sphaeroides* were shown to be correctly cleaved by a signal peptidase of *R. capsulatus* (52). The cleavage site is indicated by an arrow.

shown to induce polar or nonpolar mutations, depending on its orientation (26). The resulting mutant strains were tested for activity of the alternative nitrogenase by measuring acetylene reduction in a *nifHDK* deletion background.

Six different types of inhibition were found, and representatives of these are shown in Fig. 6. The inhibition type and the molybdenum concentration necessary to repress the alternative nitrogenase to 50% of the activity on molybdenum-free medium (IC_{50}) are given for all mutants in Table 2. No difference from the parental *nifHDK* deletion strain was found for *mopB* mutants; fourfold-higher concentrations of molybdate were necessary to inhibit the activity of the alternative nitrogenase for *modD* mutants, whereas an increase of up to 500-fold was needed for *modC*, *modB*, and *modA* mutants (Table 2). In contrast to these three types of molybdenum inhibition (types I, II, and III in Fig. 6), which still allowed complete repression of the alternative nitrogenase at sufficiently high molybdate concentrations, *mopA* mutants and *mopA mopB* double mutants could not be repressed completely (types IV, V, and VI in Fig. 6). An IC_{50} of 35 nM was determined for the *mopA* insertion mutant, able to drive expression of *modABCD* from a promoter located on the interposon (inhibition type IV). In contrast, an IC_{50} of 11 μM, which is a 1,000-fold increase compared with the parental strain (Table 2), was found for the opposite orientation of the interposon in *mopA* (type V). Even an unphysiologically high concentration of molybdate (1 mM), which had some toxic effects on *R. capsulatus*, was unable to repress the alternative nitrogenase significantly in *mopA mopB* double mutants (Table 2; inhibition type VI in Fig. 6).

TABLE 2. Molybdenum repression of the alternative nitrogenase in *mod* and *mop* mutants of *R. capsulatus*[a]

Mutant	Relevant characteristics[b]	IC_{50}[c]	Inhibition type[d]
KS36	Δ*nifHDK*	10.1 ± 3.2 nM	I
R434 BI	Δ*nifHDK modD*::Gm ▶	39.1 ± 2.5 nM	II
R434 BII	Δ*nifHDK modD*::Gm ◀	36.9 ± 4.8 nM	II
R434 AI	Δ*nifHDK modC*::Gm ▶	3.7 ± 0.3 μM	III
R434 AII	Δ*nifHDK modC*::Gm ◀	4.3 ± 0.4 μM	III
R432 I	Δ*nifHDK modB*::Gm ▶	3.5 ± 0.4 μM	III
R432 II	Δ*nifHDK modB*::Gm ◀	3.1 ± 0.1 μM	III
R438 I	Δ*nifHDK modA*::Gm ▶	4.1 ± 0.4 μM	III
R438 II	Δ*nifHDK modA*::Gm ◀	4.1 ± 0.1 μM	III
R279	Δ*nifHDK* Δ*modABCD*	4.5 ± 0.9 μM	III
R423 AI	Δ*nifHDK mopA*::Gm ▶	35.0 ± 8.2 nM	IV
R423 AII	Δ*nifHDK mopA*::Gm ◀	11.1 ± 0.7 μM	V
R423 BI	Δ*nifHDK mopB*::Gm ▶	10.1 ± 3.3 nM	I
R423 BII	Δ*nifHDK mopB*::Gm ◀	7.5 ± 0.4 nM	I
R423 CI	Δ*nifHDK* (Δ*mopAB*)::Gm ▶	>1 mM	VI
R423 CII	Δ*nifHDK* (Δ*mopAB*)::Gm ◀	>1 mM	VI

[a] The interposon insertion sites are shown in Fig. 3.
[b] Arrowheads show the direction of transcription initiated on the Gm interposon.
[c] The IC_{50} (molybdenum concentration needed to inhibit the alternative nitrogenase to 50% of the activity in Mo-free medium) was determined from at least three independent inhibition curves for each strain.
[d] Inhibition types I to VI are outlined in Fig. 6.

Proteins MopA and MopB are involved in neither molybdenum transport nor synthesis of the iron-molybdenum cofactor of nitrogenase. The data obtained from the DNA sequence and analysis of molybdenum repression of the alternative nitrogenase suggested that the gene products of *modA*, *modB*, and *modC* are involved in molybdenum transport. To test this hypothesis and to elucidate whether MopA and MopB are also involved in molybdenum transport, the activity of the conventional molybdenum-containing nitrogenase was analyzed in *modB* and *mopA mopB* double mutants (Fig. 7). To ensure that the observed nitrogenase activities were not due to the alternative nitrogenase, these two mutations were introduced into an *anfA* mutant strain of *R. capsulatus*, which is unable to express the alternative nitrogenase. As shown in Fig. 7, molybdate concentrations of >100 nM were sufficient for full activity of the molybdenum nitrogenase for the parental *anfA* mutant strain as well as for the *mopA mopB* double mutant. Therefore, MopA and MopB are not involved in the uptake of molybdenum or in the processing of molybdenum into the cofactor of the conventional molybdenum nitrogenase. In contrast, no nitrogenase activity was observed at 100 nM molybdate for the *modB* mutant. Concentrations 500-fold higher were necessary to restore full activity of the molybdenum nitrogenase in the *modB* mutant, indicating that ModB participated in high-affinity transport of molybdenum.

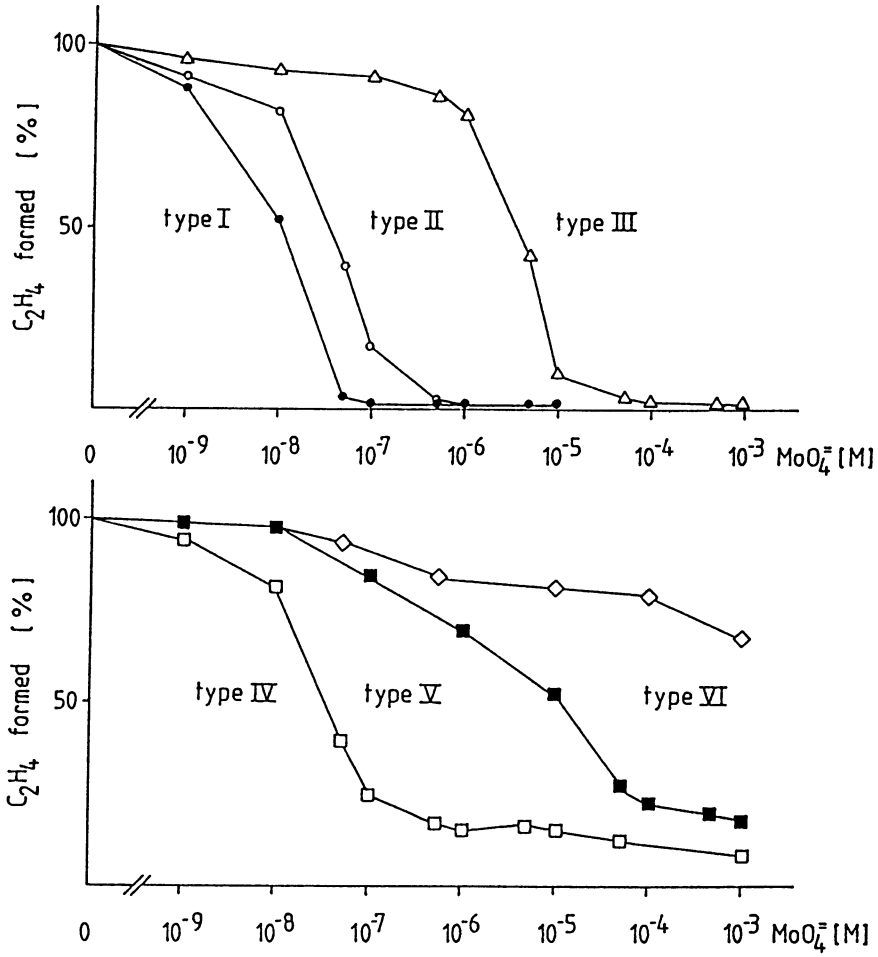

FIG. 6. Effect of increasing molybdate concentrations on the activity of the alternative nitrogenase. Representatives of all six inhibition types found for different *mod* and *mop* mutants of *R. capsulatus* (Table 2) are shown. The activity of the alternative nitrogenase was determined by the reduction of acetylene to ethylene, assayed by gas chromatography, and is expressed as a percentage of the corresponding control value in molybdenum-free medium. Type I (●) corresponds to the parental *nifHDK* deletion strain, type II (○) corresponds to a *modD* mutant, type III (△) corresponds to a *modB* mutant, type IV (□) and type V (■) correspond to *mopA* mutants carrying the interposon in different orientations, and type VI (◇) corresponds to a *mopA mopB* double deletion mutant (for details, see Table 2 and text).

DISCUSSION

DNA sequence and mutational analysis proved that at least six *R. capsulatus* genes located immediately downstream of *nifB* copy II are involved in the repression by molybdenum of the alternative nitrogenase. Two of these genes, designated *modB* and *modC*, exhibited a high degree of homology to *chlJ* and *chlD*, respectively, of *E. coli*. From the predicted secondary structure and amino acid sequence similarities to components of a variety of different transport systems, Johann and Hinton (21) suggested that ChlJ is an integral membrane protein of the molybdate transport system and ChlD is the membrane-associated ATP-binding protein responsible for energy coupling to this high-affinity transport system. Although *modA*, which was located immediately upstream of *R. capsulatus modBC*, exhibited no homology to known sequences, it seems likely that this gene encodes a periplasmic binding protein, the third component characteristic of high-affinity transport systems. The *R. capsulatus* ModA protein contained a leader sequence of 27 amino acid residues, which conformed to signal sequences of other proteins that are cleaved during translocation to the periplasm. A signal peptidase able to cleave the precursors of the *E. coli* Skp protein and *Rhodobacter sphaeroides* cytochrome c_2 at the authentic cleavage site was identified recently in *R. capsulatus* (52). From the high degree of structural and sequence similarities of the putative leader peptide of *R. capsulatus* ModA to these proteins (Fig. 5), it is likely that this signal peptidase is responsible for the export of ModA.

The same arrangement of genes coding for periplasmic binding proteins, integral membrane proteins, and ATP-binding proteins as described here for *modABC* of *R. capsulatus* was also found for the high-affinity phosphate and sulfate transport systems of *E. coli* (1, 19, 43, 47, 48). In contrast to the *R. capsulatus* molybdate transport system, these two oxyanion transport systems contained two integral membrane proteins, which exhibited significant sequence similarities to each other (1, 43, 48). The formation of a membrane complex composed of a pseudodimer of two homologous proteins was also found for a variety of other active transport systems, including the oligopeptide transport system (14) and the histidine transport system of *S. typhimurium* (12). No gene coding for a second transmembrane protein could be identified in the *R. capsulatus mod-*

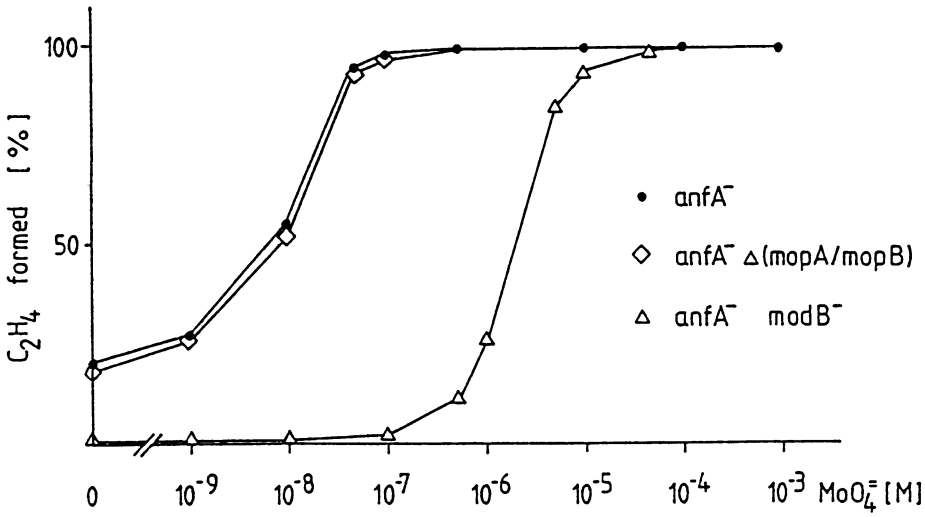

FIG. 7. Effect of increasing molybdate concentrations on the activity of the conventional molybdenum nitrogenase. The reduction of acetylene was determined by gas chromatographic methods, and the activities of the molybdenum nitrogenase are expressed as a percentage of the control value in Mo-sufficient medium. The activity of the parental *anfA* mutant strain, which is unable to express the alternative nitrogenase, is given as a control (●) and compared with the nitrogenase activities of the corresponding *modB* mutant (△) and a *mopA mopB* double mutant (◇).

ABC gene region. Therefore, it can be speculated that the integral membrane complex of the *R. capsulatus* molybdate transport system might consist of a ModB homodimer or that a gene encoding the second component is located elsewhere in the chromosome. To test this hypothesis, a *modB*-specific probe was used in Southern hybridization experiments. However, no evidence for a second copy of a *modB*-homologous gene could be obtained (data not shown).

In addition to the integral membrane components, each binding-protein-dependent transport system contains one or two ATP-binding proteins. Two such proteins are required for the oligopeptide transport system (14); a fusion protein containing two ATP-binding domains was found for the ribose transport system (6), whereas the transport systems for phosphate (1, 48) and sulfate (43) need only one ATP-binding protein, which is supposed to form a homodimer. If the organization of the *R. capsulatus* molybdate transport system conforms to the general concept emerging for active transport systems, it seems likely that both the integral membrane protein (ModB) and the ATP-binding protein (ModC) function together as homodimers. This hypothesis is corroborated by the overlapping stop and start codons of *modB* and *modC*, indicating translational coupling, which ensures equimolar amounts of both gene products (29). The same arrangement of genes coding for a single integral membrane protein and a single ATP-binding protein was found for the *sfuABC* operon of *Serratia marcescens*, which encodes a binding-protein-dependent iron transport system (3). However, the molecular weight of the membrane protein SfuB is nearly twice that of proteins usually found in binding-protein-dependent transport systems, and SfuB might originate from two fused polypeptides.

The genes encoding the structural components of the phosphate transport system are cotranscribed with *phoU*, encoding a regulatory protein involved in dephosphorylation of a transcriptional activator (for a review, see references 32 and 46), whereas the structural genes of sulfate transport are followed by *cysM*, coding for an *O*-acetylserine sulfhydrylase, which participates in cysteine biosynthesis (23, 43). The *R. capsulatus modD* gene, which is located at a comparable position downstream of *modABC*, exhibited no homology to known genes, and therefore no function could be predicted. However, it was shown (Fig. 6, Table 2) that, compared with the wild type, fourfold-higher molybdenum concentrations were necessary to repress the alternative nitrogenase in *modD* mutants, indicating that ModD is involved either in molybdenum transport or in signal transduction.

Mutations in *modA*, *modB*, and *modC* resulted in identical phenotypes. The molybdenum concentrations necessary to inhibit the alternative nitrogenase are increased 500-fold in these mutant strains. To prove the hypothesis that these genes encode the structural components of a high-affinity molybdate transport system, the activity of the conventional molybdenum-containing nitrogenase was determined. Full nitrogenase activities could be observed for *modABC* mutants only at molybdate concentrations of >50 μM, whereas >100 nM was sufficient for the wild type. This result indicated, first, that ModABC are involved in high-affinity molybdenum transport and, second, that a low-affinity system independent of *modABC* must also be present in *R. capsulatus*. This low-affinity transport system might be specific for molybdate, or more likely, other oxyanion permeases might be used to import molybdate at high concentrations. Lee et al. (24) presented data suggesting that, in the absence of the high-affinity transport system, *E. coli* utilizes sulfate transport systems for transporting molybdate. The assumption that *modABC* encode a high-affinity, binding-protein-dependent molybdate transport system would be in line with the finding that *modABC* mutants of *R. capsulatus* are still able to repress the alternative nitrogenase completely in the presence of high molybdenum concentrations, conditions which are dependent only on a low-affinity transport system. In addition, it could be concluded from these data that it is not the extracellular molybdenum concentration, detected by a putative integral membrane sensor molecule, that is responsible for molybdenum repression of the alternative nitrogenase but instead either

the intracellular molybdenum content or the activity of the transport system itself.

The *R. capsulatus modABCD* gene region is preceded by two divergently transcribed genes encoding proteins, which also exhibited homology to gene products known to be involved in molybdenum metabolism. Both MopA and MopB, two proteins with high sequence similarity, contained two domains homologous to the low-molecular-weight molybdenum-pterin-binding proteins of *C. pasteurianum*. The Mop proteins of *C. pasteurianum*, which are encoded by a multigene family (17), were shown to contain one molybdenum atom and a pterin-like compound per molecule (16). The presence of two Mop equivalents in *R. capsulatus* MopA and MopB might be an indication that these proteins are able to coordinate two molybdenum atoms and two pterins.

The expression of the alternative nitrogenase in a *mopA mopB* double mutant was independent of the molybdenum concentration (Fig. 6). This might be explained by an involvement of MopA and MopB in both the high-affinity and the low-affinity transport systems, preventing the uptake of molybdate completely. However, analysis of molybdenum uptake, measured indirectly via the activity of the conventional molybdenum-containing nitrogenase, revealed no differences between the wild type and a *mopA mopB* double mutant (Fig. 7). The analysis of single *mopA* and *mopB* mutants demonstrated that MopB can only partially substitute for MopA, because complete repression of the alternative nitrogenase could be achieved only in a $MopA^+$ background. This might be explained by the observed differences in amino acid sequences of MopA and MopB, which may account for different affinities for the substrates or for differences in interaction with other proteins.

Further experiments are now necessary to identify the components of the signal transduction pathway resulting in the repression or activation of the alternative nitrogenase and to analyze the transcriptional organization and regulation of the *R. capsulatus mod/mop* gene region.

ACKNOWLEDGMENTS

We thank K. Schüddekopf for kindly providing unpublished strains and plasmids, U. Schramm for the synthesis of oligonucleotides, S. Hennecke for excellent technical assistance, and B. Masepohl for critically reading the manuscript and helpful discussions.

This work was supported by financial grants from Deutsche Forschungsgemeinschaft (Pu 28/14-2B), from Bundesministerium für Forschung und Technologie (0319372A and 0319342A), and from Ministerium für Wissenschaft und Forschung des Landes Nordrhein-Westfalen.

REFERENCES

1. **Amemura, M., K. Makino, H. Shinagawa, A. Kobayashi, and A. Nakata.** 1985. Nucleotide sequence of the genes involved in phosphate transport and regulation of the phosphate regulon in *Escherichia coli*. J. Mol. Biol. **184:**241–250.
2. **Ames, G. F.-L.** 1986. Bacterial periplasmic transport systems: structure, mechanism, and evolution. Annu. Rev. Biochem. **55:**397–425.
3. **Angerer, A., S. Gaisser, and V. Braun.** 1990. Nucleotide sequences of the *sfuA*, *sfuB*, and *sfuC* genes of *Serratia marcescens* suggest a periplasmic-binding-protein-dependent iron transport mechanism. J. Bacteriol. **172:**572–578.
4. **Arnold, W., and A. Pühler.** 1988. A family of high-copy-number plasmid vectors with single end-label sites for rapid nucleotide sequencing. Gene **70:**171–179.
5. **Bishop, P. E., and R. D. Joerger.** 1990. Genetics and molecular biology of alternative nitrogen fixation systems. Annu. Rev. Plant Physiol. Plant Mol. Biol. **41:**109–125.
6. **Buckel, S. D., A. W. Bell, J. K. M. Rao, and M. A. Hermodson.** 1986. An analysis of the structure of the product of the *rbsA* gene of *Escherichia coli* K12. J. Biol. Chem. **261:**7659–7662.
7. **Daldal, F., S. Cheng, J. Applebaum, E. Davidson, and R. C. Prince.** 1986. Cytochrome c_2 is not essential for photosynthetic growth of *Rhodopseudomonas capsulata*. Proc. Natl. Acad. Sci. USA **83:**2012–2016.
8. **Dassa, E., and M. Hofnung.** 1985. Sequence of gene *malG* in *E. coli* K12: homologies between integral membrane components from binding protein-dependent transport systems. EMBO J. **4:**2287–2293.
9. **Donohue, T. J., A. G. McEwan, and S. Kaplan.** 1986. Cloning, DNA sequence, and expression of the *Rhodobacter sphaeroides* cytochrome c_2 gene. J. Bacteriol. **168:**962–972.
10. **Gilson, E., H. Nikaido, and M. Hofnung.** 1982. Sequence of the *malK* gene in *E. coli* K12. Nucleic Acids Res. **10:**7449–7458.
11. **Higgins, C. F., M. P. Gallagher, S. C. Hyde, M. L. Mimmack, and S. R. Pearce.** 1990. Periplasmic binding protein-dependent transport systems: the membrane-associated components. Phil. Trans. R. Soc. London **326:**353–365.
12. **Higgins, C. F., P. D. Haag, K. Nikaido, F. Ardeshir, G. Garcia, and G. F.-L. Ames.** 1982. Complete nucleotide sequence and identification of membrane components of the histidine transport operon of *S. typhimurium*. Nature (London) **298:**723–727.
13. **Higgins, C. F., I. D. Hiles, G. P. C. Salmond, D. R. Gill, J. A. Downie, I. J. Evans, I. B. Holland, L. Gray, S. D. Buckel, A. W. Bell, and M. A. Hermodson.** 1986. A family of related ATP-binding subunits coupled to many distinct biological processes in bacteria. Nature (London) **323:**448–450.
14. **Hiles, I. D., M. P. Gallagher, D. J. Jamieson, and C. F. Higgins.** 1987. Molecular characterization of the oligopeptide permease of *Salmonella typhimurium*. J. Mol. Biol. **195:**125–142.
15. **Hinton, S. M., and G. Freyer.** 1986. Cloning, expression and sequencing the molybdenum-pterin binding protein (*mop*) gene of *Clostridium pasteurianum* in *Escherichia coli*. Nucleic Acids Res. **14:**9371–9380.
16. **Hinton, S. M., and B. Merritt.** 1986. Purification and characterization of a molybdenum-pterin-binding protein (Mop) in *Clostridium pasteurianum* W5. J. Bacteriol. **168:**688–693.
17. **Hinton, S. M., C. Slaughter, W. Eisner, and T. Fisher.** 1987. The molybdenum-pterin binding protein is encoded by a multigene family in *Clostridium pasteurianum*. Gene **54:**211–219.
18. **Holck, A., and K. Kleppe.** 1988. Cloning and sequencing of the gene for the DNA-binding 17K protein of *Escherichia coli*. Gene **67:**117–124.
19. **Hryniewicz, M., A. Sirko, A. Palucha, A. Böck, and D. Hulanicka.** 1990. Sulfate and thiosulfate transport in *Escherichia coli* K-12: identification of a gene encoding a novel protein involved in thiosulfate binding. J. Bacteriol. **172:**3358–3366.
20. **Jacobson, M. R., K. E. Brigle, L. T. Bennett, R. A. Setterquist, M. S. Wilson, V. L. Cash, J. Beynon, W. E. Newton, and D. R. Dean.** 1989. Physical and genetic map of the major *nif* gene cluster from *Azotobacter vinelandii*. J. Bacteriol. **171:**1017–1027.
21. **Johann, S., and S. M. Hinton.** 1987. Cloning and nucleotide sequence of the *chlD* locus. J. Bacteriol. **169:**1911–1916.
22. **Klipp, W., B. Masepohl, and A. Pühler.** 1988. Identification and mapping of nitrogen fixation genes of *Rhodobacter capsulatus*: duplication of a *nifA-nifB* region. J. Bacteriol. **170:**693–699.
23. **Kredich, N. M.** 1987. Biosynthesis of cysteine, p. 419–428. In F. C. Neidhardt, J. L. Ingraham, K. B. Low, B. Magasanik, M. Schaechter, and H. E. Umbarger (ed.), *Escherichia coli* and *Salmonella typhimurium*: cellular and molecular biology, vol. 1. American Society for Microbiology, Washington, D.C.
24. **Lee, J. H., J. C. Wendt, and K. T. Shanmugam.** 1990. Identification of a new gene, *molR*, essential for utilization of molybdate by *Escherichia coli*. J. Bacteriol. **172:**2079–2087.
25. **Masepohl, B., W. Klipp, and A. Pühler.** 1988. Genetic characterization and sequence analysis of the duplicated *nifA/nifB* gene region of *Rhodobacter capsulatus*. Mol. Gen. Genet. **212:**27–37.
26. **Moreno-Vivian, C., S. Hennecke, A. Pühler, and W. Klipp.** 1989.

Open reading frame 5 (ORF5), encoding a ferredoxinlike protein, and *nifQ* are cotranscribed with *nifE*, *nifN*, *nifX*, and ORF4 in *Rhodobacter capsulatus*. J. Bacteriol. **171**:2591–2598.

27. **Moreno-Vivian, C., M. Schmehl, B. Masepohl, W. Arnold, and W. Klipp.** 1989. DNA sequence and genetic analysis of the *Rhodobacter capsulatus nifENX* gene region: homology between NifX and NifB suggests involvement of NifX in processing of the iron-molybdenum cofactor. Mol. Gen. Genet. **216**: 353–363.
28. **Morett, E., and M. Buck.** 1989. *In vivo* studies on the interaction of RNA polymerase-σ^{54} with the *Klebsiella pneumoniae* and *Rhizobium meliloti nifH* promoters. J. Mol. Biol. **210**:65–77.
29. **Oppenheim, D. S., and C. Yanofsky.** 1980. Tryptophan operon of *Escherichia coli*. Genetics **95**:785–795.
30. **Prentki, P., and H. M. Krisch.** 1984. In vitro insertional mutagenesis with a selectable DNA fragment. Gene **29**:303–313.
31. **Rao, J. K. M., and P. Argos.** 1986. A conformational preference parameter to predict helices in integral membrane proteins. Biochim. Biophys. Acta **869**:197–214.
32. **Rao, N. N., and A. Torriani.** 1990. Molecular aspects of phosphate transport in *Escherichia coli*. Mol. Microbiol. **4**:1083–1090.
33. **Sambrook, J., E. F. Fritsch, and T. Maniatis.** 1989. Molecular cloning: a laboratory manual, 2nd ed. Cold Spring Harbor Laboratory, Cold Spring Harbor, N.Y.
34. **Sanger, F., S. Nicklen, and A. R. Coulson.** 1977. DNA sequencing with chain-terminating inhibitors. Proc. Natl. Acad. Sci. USA **74**:5463–5467.
35. **Schneider, K., A. Müller, K.-U. Johannes, E. Diemann, and J. Kottmann.** 1991. Selective removal of molybdenum traces from growth media of N_2-fixing bacteria. Anal. Biochem. **193**:292–298.
36. **Schneider, K., A. Müller, U. Schramm, and W. Klipp.** 1991. Demonstration of a molybdenum- and vanadium-independent nitrogenase in a *nifHDK*-deletion mutant of *Rhodobacter capsulatus*. Eur. J. Biochem. **195**:653–661.
37. **Scott, D., and N. K. Amy.** 1989. Molybdenum accumulation in *chlD* mutants of *Escherichia coli*. J. Bacteriol. **171**:1284–1287.
38. **Shanmugam, K. T., V. Stewart, R. P. Gunsalus, D. H. Boxer, J. A. Cole, M. Chippaux, J. A. DeMoss, G. Giordano, E. C. C. Lin, and K. V. Rajagopalan.** 1992. Proposed nomenclature for the genes involved in molybdenum metabolism in *Escherichia coli* and *Salmonella typhimurium*. Mol. Microbiol. **6**:3452–3454.
39. **Shaw, J. G., M. J. Hamblin, and D. J. Kelly.** 1991. Purification, characterization and nucleotide sequence of the periplasmic C4-dicarboxylate-binding protein (DctP) from *Rhodobacter capsulatus*. Mol. Microbiol. **5**:3055–3062.
40. **Silver, S., and M. Walderhaug.** 1992. Gene regulation of plasmid- and chromosome-determined inorganic ion transport in bacteria. Microbiol. Rev. **56**:195–228.
41. **Simon, R., U. Priefer, and A. Pühler.** 1983. A broad host range mobilization system for *in vivo* genetic engineering: transposon mutagenesis in gram negative bacteria. Bio/Technology **1**:784–791.
42. **Simon, R., J. Quandt, and W. Klipp.** 1989. New derivatives of transposon Tn*5* suitable for mobilization of replicons, generation of operon fusions and induction of genes in gram-negative bacteria. Gene **80**:161–169.
43. **Sirko, A., M. Hryniewicz, D. Hulanicka, and A. Böck.** 1990. Sulfate and thiosulfate transport in *Escherichia coli* K-12: nucleotide sequence and expression of the *cysTWAM* gene cluster. J. Bacteriol. **172**:3351–3357.
44. **Sperl, G. T., and J. A. DeMoss.** 1975. *chlD* gene function in molybdate activation of nitrate reductase. J. Bacteriol. **122**: 1230–1238.
45. **Stewart, V.** 1988. Nitrate respiration in relation to facultative metabolism in enterobacteria. Microbiol. Rev. **52**:190–232.
46. **Stock, J. B., A. J. Ninfa, and A. M. Stock.** 1989. Protein phosphorylation and regulation of adaptive responses in bacteria. Microbiol. Rev. **53**:450–490.
47. **Surin, B. P., D. A. Jans, A. L. Fimmel, D. C. Shaw, G. B. Cox, and H. Rosenberg.** 1984. Structural gene for the phosphate-repressible phosphate-binding protein of *Escherichia coli* has its own promoter: complete nucleotide sequence of the *phoS* gene. J. Bacteriol. **157**:772–778.
48. **Surin, B. P., H. Rosenberg, and G. B. Cox.** 1985. Phosphate-specific transport system of *Escherichia coli*: nucleotide sequence and gene-polypeptide relationships. J. Bacteriol. **161**: 189–198.
49. **Vieira, J., and J. Messing.** 1982. The pUC plasmids, an M13mp7-derived system for insertion mutagenesis and sequencing with synthetic universal primers. Gene **19**:259–268.
50. **von Heijne, G.** 1986. A new method for predicting signal sequence cleavage sites. Nucleic Acids Res. **14**:4683–4690.
51. **Wang, S.-Z., J.-S. Chen, and J. L. Johnson.** 1990. A nitrogen-fixation gene (*nifC*) in *Clostridium pasteurianum* with sequence similarity to *chlJ* of *Escherichia coli*. Biochem. Biophys. Res. Commun. **169**:1122–1128.
52. **Wieseler, B., E. Schiltz, and M. Müller.** 1992. Identification and solubilization of a signal peptidase from the phototrophic bacterium *Rhodobacter capsulatus*. FEBS Lett. **298**:273–276.
53. **Yanisch-Perron, C., J. Vieira, and J. Messing.** 1985. Improved M13 phage cloning vectors and host strains: nucleotide sequences of the M13mp18 and pUC19 vectors. Gene **33**:103–119.